Vapor-liquid Phase Behavior of the Iodine-Sulfur Water-splitting Process

R. W. Bradshaw, R. S. Larson, A. E. Lutz

Sandia National Laboratories

Issued by Sandia National Laboratories, operated for the United States
Department of Energy by Sandia Corporation.

Vapor-liquid Phase Behavior of the Iodine-Sulfur Water-splitting Process

LDRD Final Report for FY03

R. W. Bradshaw
Materials Chemistry Dept. 8762

R. S. Larson
Fluid and Thermal Sciences Dept. 8752

A. E. Lutz
Hydrogen and Combustion Technology Dept. 8367

Sandia National Laboratories
P.O. Box 969
Livermore, CA 94551-0969

ABSTRACT

This report summarizes the results of a one-year LDRD project that was undertaken to better understand the equilibrium behavior of the iodine-water-hydriodic acid system at elevated temperature and pressure. We attempted to extend the phase equilibrium database for this system in order to facilitate development of the iodine-sulfur water-splitting process to produce hydrogen to a commercial scale. The iodine-sulfur cycle for thermochemical splitting of water is recognized as the most efficient such process and is particularly well suited to coupling to a high-temperature source of process heat. This study intended to combine experimental measurements of vapor-liquid-liquid equilibrium and equation-of-state modeling of equilibrium solutions using Sandia's Chemkin software. Vapor-liquid equilibrium experiments were conducted to a limited extent. The Liquid Chemkin software that was developed as part of an earlier LDRD project was enhanced and applied to model the non-ideal behavior of the liquid phases.

ACKNOWLEDGMENTS

CONTENTS

This page intentionally left blank

INTRODUCTION

The ability to produce hydrogen from water, rather than a hydrocarbon precursor, would constitute a very significant advance in the nation's energy infrastructure. To this end, the use of heat produced by a nuclear power reactor to drive thermochemical water-splitting cycles has been pursued for many years, both in the US and other countries, but no economical, large-scale process is currently available. A recent survey of thermochemical water-splitting processes by Sandia and General Atomics evaluated more than 100 thermochemical cycles and concluded that the iodine-sulfur water-splitting cycle is the most efficient in using a thermal energy input.[1] The temperature requirements of the iodine-sulfur cycle are also well suited to coupling to a high-temperature nuclear power reactor to provide process heat.

The iodine-sulfur water-splitting cycle involves a number of process steps consisting of chemical reactions and physical separations. The primary step is the reaction of water, sulfur dioxide and iodine to produce hydriodic acid (HI) and sulfuric acid. Many subsequent steps are necessary, but particularly important are the steps in which these products are separated, and, in which HI is subsequently dissociated to yield hydrogen and iodine. Other process steps complete a closed loop into which only water and heat enter and hydrogen (and oxygen) exits. Key separation steps involve the removal of HI and I_2 from sulfuric acid and the removal of HI from I_2 and water. Both separations are designed as distillation processes that occur at elevated temperature and pressure. Thus, information regarding the vapor-liquid equilibrium is necessary to design this key separation stage. We focussed on the phase behavior concerning the separation of HI from iodine and water in this project.

The vapor-liquid equilibria relevant to these separation steps have not been characterized adequately for process design and cost estimation. Vapor-liquid equilibrium experiments will be conducted for the system iodine-hydriodic acid-water, at elevated temperature (up to 250°C) and pressure (up to about 400 psi) relevant to the iodine-sulfur process. The formulation of a real-gas equation of state will extend the applicability of the laboratory data to a wider range of process design calculations concerning the iodine separation step in the overall process. This key physical property correlation will have a significant impact on advancing the technology of producing hydrogen from the excess heat of nuclear reactors.

Only a few studies have been conducted to map the HI-I_2-H_2O phase diagram at conditions relevant to a practical process. General Atomics investigated the liquid-liquid-vapor equilibrium in 1984 using a novel technique they called the isopiestic method, which employed a sealed quartz vessel having two liquid compartments and a connecting vapor channel.[2] Vapor pressure data were not obtained and the compositions of the liquid phases were deduced from volumetric measurements rather than by sampling and chemical analysis. Experiments at the Univ. of Aachen (Germany) measured the vapor pressure over a wide range of overall composition, but did not determine the composition

of the vapor or the co-existing liquid phases.[3,4] Experiments have also been reported recently by Sakurai for the H_2SO_4-HI-I_2-H_2O system, although at temperatures below 95°C and essentially atmospheric pressure.[5] A similar low-temperature study of the related system based on bromine, rather than iodine, has been published by Ishikawa and co-workers.[6]

Scope of LDRD Study

Given the limitations of previous experimental work, we planned to obtain phase diagram information using a pressure vessel constructed of materials that are compatible with HI, iodine and water, when operated at temperatures up to approximately 250°C. This information would include vapor pressure (up to several hundred psi) and the compositions of the three phases known to exist for this system (2 liquid and vapor) as a function of temperature and overall composition. Accomplishing these measurements required designing, constructing and operating a pressure cell with appropriate phase mixing to achieve thermodynamic equilibrium conditions in a highly corrosive environment.

Computational models were used to interpret experimental phase diagram data with the aim of extending the range of temperatures and pressures at which that data may be used to design the production-scale process. We adapted Sandia's Chemkin software to model the phase equilibrium of the HI-I_2-H_2O system. The original Chemkin interface to the STANJAN equilibrium solver allowed only for use of the Surface Chemkin routines that consider heterogeneous mixtures of ideal gas and bulk (or liquid) phases. Later, the equilibrium code was provided with an optional link to the Chemkin Real-Gas routines, developed in a joint effort between Sandia and Professor P. B. Butler at U. of Iowa. In this project, the equilibrium code was further enhanced by adding a link to the Liquid Chemkin package, thereby making possible the simulation of systems involving nonideal liquid mixtures. In addition, a new routine describing the thermodynamics of mixtures containing both ions and nonelectrolytes was added to Liquid Chemkin itself. Both of these improvements were necessary to allow modeling of the HI-I_2-H_2O system.

EXPERIMENTAL APPROACH, RESULTS, AND DISCUSSION

Equilibrium cell apparatus

The determination of the HI-I_2-H_2O phase equilibria at elevated temperatures and pressure presents significant challenges with regard to experimental design, operation and sampling of phase constituents. The primary issue concerning the experimental apparatus is to establish and maintain equilibrium conditions in a system of chemical constituents that are very corrosive to most pressure vessel construction materials. Furthermore, the iodine-hydriodic acid-water system forms two liquid phases and a vapor phase. The liquid phases partition into a dense iodine-rich phase (specific gravity more than 3) and a lighter water-rich phase. Withdrawing representative samples of the three equilibrated phases without compromising the fidelity of the samples is another practical concern for such experiments.

The design approach chosen for the HI-I_2-H_2O experimental apparatus was based on an equilibrium cell described by Watts at NIST.[7] The NIST equilibrium cell is designed to maintain isothermal conditions at elevated temperature for the prolonged periods required to assure that the phases are equilibrated. The cell is primarily intended for aqueous salt solutions mixed with organic compounds, which are significantly less corrosive than HI-I_2-H_2O. The apparatus consists of a heavy-wall pressure vessel enclosed in aluminum blocks, to minimize thermal transients, inside a large thermostatically-controlled oven. Recirculation of the liquid and vapor phases is essential to attain thermodynamic equilibrium within a reasonable period of time. The liquid phase is recirculated by a piston-type pump and the vapor phase is recirculated by a magnetically-driven positive displacement pump that is located within the oven. The cell is instrumented with platinum resistance thermometers for highest accuracy and precision and with quartz pressure transducers. Additionally, vibrating tube densimeters are used to measure the density of each phase at temperatures below about 140°C. Samples of the liquid phase are drawn from the recirculated stream into an external reservoir. The vapor phase is sampled by a multi-port valve that conveys the vapor to a gas chromatograph.

Pressure cell design

The approach to building the apparatus for this LDRD was to follow the guidelines of the above apparatus with modifications necessary to accommodate the corrosive environment of the water-iodine-hydriodic acid system, the existence of two liquid phases, and the large difference in density between the two liquid phases formed. Significant difficulties were anticipated regarding the means to recirculate the liquid phases. An alternative design was considered, based on the work of Knoche et al., who used a glass-lined pressure vessel to study the decomposition of HI (with water and iodine present) to hydrogen, [4] but procurement problems, among others, precluded this approach for this project.

A Model HR-100 pressure vessel rated to 4300 psi at 250°C was obtained from Berghoff America, Coral Gables, FL. The vessel was constructed from SS316 with a PTFE liner to prevent contact of the metallic surfaces with the corrosive environment. The vessel head was sealed with a PTFE O-ring compressed by a proprietary clamping fixture.

The internal volume was 100 ml and a PTFE-coated thermocouple sheath was provided for temperature measurements. The vessel was acquired with a single liquid sampling downcomer that was connected to a PTFE-coated valve on the vessel head. A pressure gauge was supplied by the manufacturer to indicate pressure, but did not have suitable accuracy for thermodynamic measurements. This vessel was capable of being stirred by a PTFE -coated stir bar driven inductively by an external stirrer. The vessel was obtained late in the year and it was not possible to engineer the considerable number of external sampling lines, valves, sample receivers, etc. within the time period of the program. Further difficulties were encountered in identifying suppliers for the ancillary equipment because of the necessity to have either corrosion-resistant metallic items (e.g., tantalum) or PTFE-coated surfaces throughout where contact with the iodine-hydriodic acid-water environment was possible for more than a short period of time.

Pressure cell design – recommendations
In view of the difficulties encountered in procuring and building the experimental apparatus for this LDRD, and drawing upon information uncovered in the technical literature relatively late in this project, the following recommendations may assist future efforts in this area. The choice of materials of construction is the major issue. Quartz and Pyrex glass have been shown to be chemically compatible with HI-I_2-H_2O at temperatures up to 250°C for at least 1200 hours.[4] Because these materials do not have sufficient mechanical strength to support the pressure loads generated in this system, they may be used as liners, although that approach creates problems because similar materials must be available for all the ancillary components as well as the pressure vessel.

A design approach that merits serious consideration is a balanced-pressure cell, in which an inner vessel of compatible material is enclosed in an outer vessel that serves as the pressure boundary. The interstitial volume is maintained at a pressure equal to the vapor pressure of the system being studied. Thus, the stress on the containment vessel is small and materials such as quartz or Pyrex glass can be used to fabricate it. The vapor pressure must be measured regardless as it constitutes a key property of the phase diagram. This approach also allows flexibility in the choice of materials for sampling lines because they do not support pressure loads. Sampling tubing can be terminated at feedthroughs in the pressure vessel boundary that connect to lined alloy tubing externally, which is capable of supporting the unbalanced loads. These internal lines can be PTFE tubing, adjusted to terminate in each of the liquid phases as well as the gas phase.

A potentially useful pressure measurement method follows from the work of Wuster et al. [8] The vapor pressure can be measured by a quartz Bourdon tube fused into the wall of a quartz or Pyrex equilibrium cell. The deflection of the tube can be detected by reflected light [8] or by continuity changes in an electrical circuit, which is potentially a simpler and more robust method. The deflection of the tube can be 'zeroed' by adjusting the external balancing pressure. This pressure can be measured straightforwardly and very accurately without the constraints arising from a corrosive environment.

Mixing of the phases within a balanced pressure vessel requires an approach that ensures that both liquid phases are dispersed in the vapor and each other. A suggested method is

to use a magnetically-driven, reciprocating quartz bucket that has a driven magnet enclosed within a quartz tube that contains the experimental environment and a driving magnet that is activated by a suitable mechanism in the balanced-pressure volume. If the bucket is fabricated with appropriate drainage holes, portions of both liquid phases can be raised into the vapor space and establish dropwise interphase contact during drainage. Repetitive cycles would assure good mixing. Such an arrangement would avoid problems that might arise when attempting to stir two liquid phases that have a large difference in density.

The primary disadvantage of a balanced-pressure cell is complexity in arranging loading and sampling. However, such an approach has been used by Knoche et al. [4] to measure vapor pressures in the HI-I$_2$-H$_2$O system, albeit without access for removing samples of the equilibrated phases.

Pyrex cell for low pressure tests
A Pyrex pressure vessel apparatus was used for a few preliminary experiments. The vessel was an Ace Glass Pressure Reactor Model 6436 rated to 50 psig, having a volume of 500ml and 5 access ports. Ace Glass PTFE threaded fittings with FPTFE O-rings were used to seal fittings and feed-throughs. A schematic and photograph of the assembled cell is shown in Figure 1. The vessel was stirred by a PTFE-coated magnetic stir bar driven externally to the pressure flask by a variable-speed magnetic stirrer. The stirrer was located within the heated cavity of the oven and operated at temperatures up to 135°C reliably. This simple mixing arrangement was not expected to be adequate for thermodynamic measurements but allowed preliminary experiments to be performed. A Pyrex thermocouple well was used to insert a Type K thermocouple beneath the liquid level in the vessel. The photograph in Figure 2 shows a close-up view of the vessel and components. Effective sealing at temperature was accomplished using Ace-Thred plugs and feedthroughs with FPTFE O-rings. The suitability of these seals was verified at temperatures up to 130°C with a helium-water load in the vessel, to create nominal system vapor pressures, before experimenting with HI and iodine. A sampling tube was placed in the water-rich liquid phase. This line consisted of PTFE tubing, sealed with a PTFE ACE-Thred compression fitting and a FPTFE O-ring. A Kalrez stopcock was used as sampling valve, as shown projecting from the upper left of the vessel in the photograph in Figure 1. PTFE tubing was also used to connect the test cell to a 0-50 psig pressure gauge located outside the oven.

Samples of liquid from the water-rich phase were removed from the pressure vessel and discharged into a receiver vessel immersed in an ice bath. The sampling line was back-pressured with argon, to a total pressure about 1 psi less than that of the system vessel. This method enabled the discharge rate of the liquid to be controlled by the stopcock in the sampling line to assure slow delivery. The free volume of the sampling line tubing was reduced to the minimum possible by sleeving it with PTFE tubing of smaller diameter.

Pyrex cell screening tests

A few preliminary experiments were conducted using water-rich HI-I_2-H_2O mixtures, mainly for familiarization with the techniques of handling hydriodic acid and iodine. These observations are presented here recognizing that it is unlikely that equilibrium was achieved during the period of the experiments despite the observation that the system pressure remained constant for at least one hour at a constant cell temperature. The assembled apparatus was loaded with water, hydriodic acid (55%, unstabilized, Sigma-Aldrich) and a small amount of iodine. The proportions of the constituents were not intended to simulate those expected at process conditions. The cell was flushed with nitrogen in a glove bag before the experimental mixture was loaded. The cell was plugged and transferred to the oven, where it was slowly purged with helium while fitting connections were made. A leak check was performed at a nominal pressure of 25 psig before heating the oven. The cell was heated to temperatures of approximately 120°C to 135°C and held at a constant temperature for an hour before sampling. The test temperatures were limited to 120°C and total pressures less than 30 psig because of the physical limitations of the Pyrex vessel. The compositions of the water-rich liquid phase samples were analyzed for iodine content using the analytical procedure, Method 8031, specified for the Hach Model DR2010 Spectrophotometer.[9]

The compositions of the mixtures tested and the nominal values of vapor pressure are collected below. Although little change in vapor pressure was observed in these few experiments, the differences in the amount of iodine in the vapor phase were visually obvious among the tests. Figures 2 and 3 show photographs of the pressure cell at operating temperature for mixtures B and A, respectively. The overall compositions of these mixtures are given in Table 1. The color density of the vapor phases in is due to the deep purple color of iodine. Comparing these two photos shows that more vaporized iodine is present in mixture A (Fig. 3) . This is expected qualitatively because mixture A had less HI, thereby reducing the amount of iodine retained in the water-rich phase as tri-iodide.[2]

Table 1. Observations from Pyrex cell screening tests. The balance of the constituents was water.

Mixture	Iodine (wt. %)	HI (wt. %)	Temp. (°C)	Vapor Pressure (atm)	Iodine in Water-rich phase (ppm)
A	0.68	0.15	111.1	1.29	690
B	0.56	10.3	114.4	1.25	4630
B	0.56	10.3	115.0	1.28	11600
C	4.7	22.6	116.7	1.21	33800

COMPUTATIONAL MODELING

The goal of the computational modeling part of this project is to develop the capability to construct phase diagrams of the type needed in describing the behavior of the HI-I_2-H_2O system. This is to be accomplished by making suitable enhancements to the Chemkin [10] package of codes that was originally developed at Sandia. Although Chemkin has long been used to solve a wide variety of problems involving the thermodynamics and kinetics of chemically reacting systems, it has not been used to model the behavior of coexisting condensed phases, principally because it has not had the ability to describe the thermodynamics of nonideal liquid mixtures. A first step in overcoming this limitation was taken with the introduction of a new Liquid Chemkin package as part of a previous LDRD project [11]. Like the original gas-phase Chemkin and the Surface Chemkin package added later, Liquid Chemkin consists of an Interpreter program that reads user-supplied input data and a subroutine library that can be accessed by an application code to provide needed physical properties. The properties made available by the first version of Liquid Chemkin were activity coefficients and thermodynamic functions for three different kinds of nonideal liquid mixtures. However, it is still not possible to construct the kinds of phase diagrams needed here, because a suitable application code does not exist. Such a code must be able to compute the compositions of all phases coexisting at equilibrium under given conditions of temperature and pressure. While the Chemkin package does contain an equilibrium code (EQUIL), the latter has no interface to Liquid Chemkin and thus cannot handle nonideal liquids. Perhaps just as important, EQUIL is basically an interface to the standard solver STANJAN [12], whose sophisticated algorithms are designed to take advantage of the special mathematical properties of ideal mixtures. Thus, there is no certainty that EQUIL will be able to perform the necessary computations even when access to Liquid Chemkin is implemented. Finally, it is highly unlikely that the thermodynamic behavior of the phases in the HI-I_2-H_2O system can be well represented by the rather simple models included in the existing version of Liquid Chemkin. All of these obstacles must be overcome in order to achieve the goals of the current project.

In light of the above, it is logical to adopt a four-step approach to obtaining a set of codes that can do the necessary computations:
(1) Adapt the EQUIL code and its STANJAN-based subroutines to make use of the physical properties provided by the Liquid Chemkin subroutine library. This will involve not only the purely mechanical task of setting up the necessary links, but also the replacement of certain subroutine calls in STANJAN with calls to the more general routines in Liquid Chemkin.
(2) Use the newly modified EQUIL code to construct some representative phase diagrams based on the nonideal-liquid models currently existing in Liquid Chemkin. This will be the first demonstration that the Chemkin suite can model the kinds of complex phase behavior associated with nonideal liquid mixtures, in particular the existence of azeotropes and the phenomenon of phase splitting.
(3) Add to Liquid Chemkin the model needed to represent the thermodynamic properties of HI-I_2-H_2O mixtures. Although Liquid Chemkin already has some ability to

handle ionic (electrolyte) solutions and nonideal mixtures of nonelectrolytes, a model that addresses both of these complexities simultaneously is needed here.

(4) Using the thermodynamic model adopted in step (3), compare the results of EQUIL computations with experimental data in order to evaluate any unknown parameters for the HI-I_2-H_2O system. Once these parameters are known, the construction of a complete phase diagram should in principle be possible.

The details involved in carrying out these steps and the results achieved will now be summarized.

Coupling of EQUIL with Liquid Chemkin

The mechanical aspects of linking EQUIL with Liquid Chemkin are fairly straightforward. The driver program EQDRIV now opens the linking file created by the Liquid Chemkin Interpreter and makes it available to the main EQUIL code. The latter sets up the Liquid Chemkin work arrays, thereby allowing access to the routines in the Liquid Chemkin subroutine library. The call lists for many of the routines in EQUIL and STANJAN have been expanded to include the new work arrays, as necessitated by the hierarchy in which the routines are called.

Existing calls in EQUIL and STANJAN to thermodynamic property routines from Surface Chemkin have been replaced by corresponding calls to Liquid Chemkin routines, since the latter are more general and include the former as a special case. In addition to this, however, several new calls have been inserted at various points in STANJAN. In order to see why this was done, a short digression about the solution procedure used in STANJAN is necessary.

For a system at a specified temperature and pressure, STANJAN finds the equilibrium composition by minimizing the total Gibbs free energy G with respect to the species mole numbers n_j, subject to constraints on the atom populations. The constraints are handled via the method of Lagrange multipliers, which requires that variations dG corresponding to arbitrary variations dn_j be calculated. For a given phase, the free energy is

$$G = \sum_j n_j \mu_j = \sum_j n_j \left[\mu_j^0(T,P) + RT \ln x_j \right] \qquad (1)$$

where the μ_j are chemical potentials and the x_j are mole fractions. The second equality is specific to an ideal mixture and is the form assumed by STANJAN. The variation dG at constant T and P is then easily shown to be

$$dG = \sum_j \left[\mu_j^0(T,P) + RT \ln x_j \right] dn_j \qquad (2)$$

For a nonideal mixture, on the other hand, dG must be written more generally as

$$dG = \sum_j \mu_j dn_j + \sum_j n_j d\mu_j \qquad (3)$$

14

However, the second term on the right-hand side is always zero, by the Gibbs-Duhem equation, regardless of whether the mixture is ideal. It follows that Eq. (2) is also valid for a nonideal phase, *except* that the so-called standard state chemical potential must now be allowed to be a function of the composition variables. This quantity is simply *defined* to be the actual chemical potential minus the contribution from the ideal entropy of mixing. The fact that it varies with composition accounts for the need to re-evaluate it in STANJAN at points where such a calculation would otherwise be unnecessary, due to the constancy of T and P. A new routine SJTPX has been added to STANJAN in order to facilitate these calculations. This procedure should ensure that any solution returned by STANJAN does indeed correspond to a minimum in the Gibbs energy. However, since the iteration schemes in STANJAN undoubtedly take advantage of the form of the ideal solution equations to some extent, it is quite possible that the convergence properties of the code will be degraded in this more general application. In other words, the code is likely to run slower and may not be able to find a solution at all.

Sample Calculations and Phase Diagrams

With the newly-modified EQUIL and STANJAN, it is now possible to construct some representative phase diagrams using the nonideal solution formulations already existing in Liquid Chemkin. The most convenient formulation for this purpose is the regular solution model based on a theory developed by Scatchard and Hildebrand and well-summarized by Prausnitz [13]. This is applicable to a mixture of nonelectrolytes and expresses the nonidealities in terms of two parameters, namely the solubility parameter and the liquid molar volume, for each species. Although the model is mathematically simple, it is also quite versatile; in particular, it has the ability to predict phase splitting in mixtures of chemically dissimilar components. Using the equations given by Prausnitz [13], it can be shown that a system will exhibit such behavior if the following condition is satisfied:

$$\frac{2v_2(\delta_1 - \delta_2)^2}{RT} > \frac{1}{m}\left[(1 - m + m^2)^{1/2}(2m^2 - 2m + 2) + (m + 1)(m - 2)(1 - 2m)\right] \qquad (4)$$

Here the δ_j are solubility parameters, the v_j are molar volumes, and m is the ratio of v_2 to v_1. To take two examples, if parameter values from Prausnitz [13] are used, then a mixture of n-pentane and carbon disulfide at 298 K does not satisfy Eq. (4), but a mixture of neopentane and liquid bromine does. Therefore, a comparison of the phase diagrams predicted by EQUIL and Liquid Chemkin for these two systems should provide an interesting test of the new equilibrium code.

Computational results for the n-pentane/carbon disulfide system are shown in Figure 4. For the fixed temperature of 298 K and for various combinations of total pressure and overall system composition, EQUIL was asked to determine the compositions and relative amounts of all phases coexisting at equilibrium. Allowance was made for the possibility of two liquid phases as well as a vapor phase; however, as can be seen, there is never more than one liquid phase present, in agreement with the prediction of Eq. (4). It

15

should be noted that the vapor phase properties were calculated with the original Chemkin rather than the more recently developed Real Gas Chemkin; at the low pressures prevailing here, this should be entirely adequate. In any case, it can be seen that the dew point (red) and bubble point (blue) curves meet not only at the pure-component boundaries, but also at an intermediate composition of about 58% n-pentane, where the vapor pressure is maximized. This is a typical minimum-boiling azeotrope and is not unexpected for two components whose individual boiling points do not differ greatly. The points on the two curves represent actual values computed by EQUIL; the fact that there are no points in the immediate vicinity of the azeotrope is important, because it signifies that the code fails to converge in this region. This confirms the earlier speculation that the new version of EQUIL might not be as robust as the original.

Figure 5 shows the corresponding results for the neopentane-bromine system; an expanded view of the left side of the diagram is shown in Figure 6. Obviously, the prediction that this system will exhibit liquid-liquid phase splitting is confirmed. In fact, while liquid neopentane can dissolve a modest amount of bromine, the bromine-rich phase contains very little neopentane. The compositions of the two phases, which are independent of pressure in this approximation, have been verified by an independent manual calculation involving minimization of the Gibbs free energy. Of course, the quantitative details are not important for the problem at hand, other than to show that the new EQUIL appears to be working properly. The complexity of the diagram, involving six separate regions and three phase boundaries with discontinuous slopes, is in sharp contrast to the result obtained by simply equating the solubility parameters and thus ignoring the nonidealities. This produces the diagram in Figure 7, which could have been obtained more directly by applying Raoult's law to both components. In short, the new EQUIL is capable of modeling complex phase behavior for at least some kinds of liquid-phase nonidealities. Again, however, it should be noted that the computations often fail to converge near points where several phases coexist.

Addition of Electrolyte NRTL Model to Liquid Chemkin

With the basic capabilities to construct complex phase diagrams now demonstrated, the next step is to add to Liquid Chemkin a new thermodynamic model that can reproduce the behavior of the HI-I_2-H_2O system. As noted above, such a model must allow for the simultaneous existence of electrolytes and chemically incompatible nonelectrolytes. An excellent candidate, as suggested by Mathias and Brown [14], is the electrolyte NRTL (nonrandom two-liquid) model developed by Chen and co-workers [15,16]. This is basically a fusion of the original NRTL model for nonelectrolytes (see Prausnitz [13]) with the Pitzer-Debye-Hückel model for ionic solutions. In its most general form, this model gives rise to extremely cumbersome equations for the activity coefficients, so the present work will deal only with a special case, and the details of the derivations will be omitted.

For the HI-I_2-H_2O system, the only ions expected to be present are H_3O^+ and I^-, so the ElecNRTL equations will be written for the case of a single cation and a single anion but

any number of molecular components. The expressions for the local (short-range) contribution to the activity coefficient are [16]

$$\ln \gamma_m^{lc} = \frac{S_m}{R_m} + \sum_n \frac{X_n G_{mn}}{R_n}\left(\tau_{mn} - \frac{S_n}{R_n}\right) + \frac{X_c G_{mc,ac}}{R_{ac}}\left(\tau_{m,ca} - \frac{S_{ac}}{R_{ac}}\right) + \frac{X_a G_{ma,ca}}{R_{ca}}\left(\tau_{m,ca} - \frac{S_{ca}}{R_{ca}}\right) \qquad (5)$$

$$\frac{1}{Z_c}\ln \gamma_c^{lc} = \frac{S_{ac}}{R_{ac}} + \sum_m \frac{X_m G_{ca,m}}{R_m}\left(\tau_{ca,m} - \frac{S_m}{R_m}\right) - \frac{X_a S_{ca}}{R_{ca}^2} - \tau_{w,ca} - G_{ca,w}\tau_{ca,w} \qquad (6)$$

$$\frac{1}{Z_a}\ln \gamma_a^{lc} = \frac{S_{ca}}{R_{ca}} + \sum_m \frac{X_m G_{ca,m}}{R_m}\left(\tau_{ca,m} - \frac{S_m}{R_m}\right) - \frac{X_c S_{ac}}{R_{ac}^2} - \tau_{w,ca} - G_{ca,w}\tau_{ca,w} \qquad (7)$$

where

$$S_m = \sum_k X_k G_{km}\tau_{km} \qquad (8)$$

$$R_m = \sum_k X_k G_{km} \qquad (9)$$

$$S_{ac} = \sum_m X_m G_{mc,ac}\tau_{m,ca} \qquad (10)$$

$$R_{ac} = X_a + \sum_m X_m G_{mc,ac} \qquad (11)$$

$$S_{ca} = \sum_m X_m G_{ma,ca}\tau_{m,ca} \qquad (12)$$

$$R_{ca} = X_c + \sum_m X_m G_{ma,ca} \qquad (13)$$

$$G_{jm} = \exp\left(-\alpha_{jm}\tau_{jm}\right) \qquad (14)$$

$$G_{ji,ki} = \exp\left(-\alpha_{ji,ki}\tau_{ji,ki}\right) \qquad (15)$$

In these equations the subscripts j and k refer to any species, while m and n refer specifically to a molecular (nonionic) species, i to an ionic species, c to the cation, and a to the anion. The subscript w denotes the principal solvent, presumably water, which is used in defining the standard state for the ions. Specifically, the activity coefficient for each ion is unity in an infinitely dilute solution of the ions in solvent w, whereas the activity coefficient for a molecular species is unity for that species in its pure state. This

is the so-called unsymmetric convention for activity coefficients, which is used for compatibility with the long-range contribution to be discussed below.

Returning to Eqs. (5)–(15), Z_k is the absolute value of the charge on species k, while X_k is a modified mole fraction obtained by multiplying the true mole fraction by Z_k if the species is ionic or by unity if the species is molecular. The various α and τ values are nonrandomness factors and dimensionless interaction energies, respectively, and are the basic parameters for this part of the ElecNRTL model. Although there are at first glance a great many of these, arguments given in [16] can be used to reduce drastically the number of independent values. First of all, the α matrix for molecular components is symmetric, and all α values involving ions are taken to be equal. Furthermore,

$$\tau_{cm} = \tau_{am} \equiv \tau_{ca,m} \tag{16}$$

$$\tau_{ma,ca} = \tau_{mc,ac} \equiv \tau_{m,ca} \tag{17}$$

and Eq. (16) also applies with τ replaced by G. The list of necessary parameters is thus reduced to

$$\alpha_{ca,m}, \quad \alpha_{nm}, \quad \tau_{ca,m}, \quad \tau_{nm}, \quad \tau_{m,ca} \tag{18}$$

for all values of n and m.

The expression for the Pitzer-Debye-Hückel (long-range) contribution to the activity coefficient is considerably simpler. For any species k,

$$\ln \gamma_k^{PDH} = -\frac{1}{3}\left(\frac{2\pi N_0 d}{M_s}\right)^{1/2}\left(\frac{e^2}{DkT}\right)^{3/2}\left[\frac{2Z_k^2}{\rho}\ln\left(1+\rho I_x^{1/2}\right)+\frac{Z_k^2 I_x^{1/2}-2I_x^{3/2}}{1+\rho I_x^{1/2}}\right] \tag{19}$$

where I_x is the ionic strength on a mole fraction basis:

$$I_x = \frac{1}{2}\sum_i Z_i^2 x_i \tag{20}$$

N_0 is Avogadro's number; d, M_s, and D are the density, molecular weight, and dielectric constant of the solvent, respectively; e is the elementary charge; k is Boltzmann's constant; and ρ is the closest approach parameter, which is generally set equal to 14.9. The quantity multiplying the square brackets in Eq. (19) is basically a property of the solvent, which is generally not a pure species, so appropriate averages must be computed. In the absence of information to the contrary, a molar average is used for the dielectric constant.

The implementation of the ElecNRTL model in Liquid Chemkin requires changes to both the Interpreter and the subroutine library. Actually, the declaration of a given phase as being of this type (keyword NRT) occurs in the input file to Surface Chemkin; however, this requires no changes to the latter, and this information is simply passed to Liquid Chemkin via the Surface Chemkin linking file. The Liquid Chemkin Interpreter now recognizes NRT as a valid phase formulation and checks to make sure that no conflicting formulation (such as DEB, REG, or SER) has been declared for the same phase. It also checks to see that all necessary model parameters have been supplied in the Liquid Chemkin input file. The values that must be provided include those in (18) above as well as D and ρ for each of the molecular species. All of this checking is done in a new routine LKCNRT. It should be noted that the density for each molecular species is declared as always in the *Surface* Chemkin input file. While this information is regarded by the Surface Chemkin Interpreter as optional and will not generate an error or even a warning if omitted, it obviously is necessary input if the ElecNRTL model is used.

A few other technical details should also be mentioned. In the species declarations for an NRT phase in the Surface Chemkin input file, the cation (if any) must be listed first and the anion second, followed by the molecular species. There is no danger of erroneous results if this rule is violated, because the Liquid Chemkin interpreter will note the violation and generate an error condition. Also, the principal solvent, as defined above, must be the last species declared; this is the means of identifying this species to Liquid Chemkin, so violating this rule will indeed lead to erroneous results. However, the output file from the Liquid Chemkin Interpreter contains a note identifying the primary solvent, so inadvertent errors should be obvious to the user. Finally, when the same chemical species appears in two (or more) different phases having the same formulation type, that species must be given a different name in each phase. This is a result of the fact that Chemkin assigns to each species in each phase a unique species index. When the Liquid Chemkin input file is read by the Interpreter, data for a given species name is assigned to the first species index corresponding to that name; therefore, any other index corresponding to the same name will have no data, and the Interpreter will report an error.

The activity coefficient for any species in an NRT phase is obtained by summing the contributions from Eq. (5), (6), or (7), as appropriate, and (19). These computations are carried out in the new routine LKNRT contained in the Liquid Chemkin subroutine library. However, a very important caveat with regard to this routine must be mentioned. Since the temperature derivatives of Eqs. (5)–(7) are extraordinarily complicated, they are not currently evaluated in LKNRT. (The complexity arises principally from the fact that the τ values are at best inversely proportional to T.) Of course, there is then no purpose in including temperature derivatives of Eq. (19). For these reasons, the partial molar enthalpies, heat capacities, and entropies for the species in an NRT phase are not currently computed reliably by Liquid Chemkin, as can be seen from Eqs. (3.27)–(3.29) of Reference [11]. Fortunately, however, the temperature derivatives cancel when partial molar Gibbs free energies (i.e., chemical potentials) are evaluated, so these quantities should be correct. Therefore, as long as EQUIL and STANJAN deal only with free energies and not with enthalpies and entropies separately, the results of the equilibrium

computations should be reliable. Of course, the regular solution calculations described earlier are not subject to this issue.

The Liquid Chemkin subroutine library also contains several new routines that are not specifically related to the ElecNRTL model. The routine LKS0ML returns a set of partial molar entropies from which the contribution due to the ideal entropy of mixing has been removed. The need for this can be inferred from the discussion following Eq. (3) above. Both LKS0ML and the previously existing LKSOR now call a new routine LKLNG which provides the logarithms of the activity coefficients directly; this is preferable to calling LKACOF and then taking the logarithms, because it eliminates unnecessary computations and lessens the chance for overflows. Finally, the new routines LKGML and LKGBML return partial molar Gibbs free energies (chemical potentials) and molar-average Gibbs energies, respectively. These have been added solely for convenience, but their usefulness in investigating questions of equilibrium should be evident.

Phase Behavior of the HI-Iodine-Water System

The one remaining task is to evaluate the ElecNRTL parameters for the $HI-I_2-H_2O$ system and to use them in constructing a phase diagram. For the moment, attention will be focused on liquid-liquid equilibria (LLE), so that the complexities involved in dealing with a nonideal vapor phase can be deferred. A set of tentative ternary phase diagrams based on limited experimental data is given by O'Keefe et al. [2], and a preliminary attempt to model some of them using Aspen software has been reported by Mathias and Brown [14]. Here an attempt will be made to use the newly enhanced Chemkin package to reproduce the experimental diagram at 393 K and 4.3 MPa. Under these conditions there are two distinct two-phase domes separated by a large region of complete miscibility, as shown in Figure 8. This should provide a reasonable test of the new software.

One of the distinct advantages of the ElecNRTL model is that it expresses multicomponent thermodynamic properties entirely in terms of binary parameters. It is therefore logical to use binary experimental data whenever possible to evaluate the parameters for the overall system. For a true ternary system, there are of course only three distinct pairs of components. The present situation is made more complicated by the fact that there is a dissociation reaction, namely

$$HI + H_2O \Leftrightarrow H_3O^+ + I^- \tag{21}$$

that increases the number of species by two (although electroneutrality demands that the concentrations of the two ions be equal.) Of course, the existence of a chemical reaction is irrelevant to an equilibrium code, but the existence of the additional species must certainly be taken into account. In accordance with the rules set out above for declarations in the Surface Chemkin input file, the species will be numbered as follows:

1. H_3O^+

2. I^-

20

3. I_2
4. HI
5. H_2O

From the phase diagram in Figure 8, it appears that HI and I_2 are miscible in all proportions, so there is little to be gained by investigating this molecular pair. On the other hand, I_2 and H_2O exhibit very limited miscibility. From the charts in [14], the mole fraction of I_2 in the H_2O-rich phase is only 6.01×10^{-4} at 393 K, while the mole fraction of H_2O in the I_2 phase is 0.0200. These are the values to be matched by adjusting ElecNRTL parameters in the EQUIL calculations. Following a suggestion in [16], the number of adjustable parameters can be minimized by setting all nonrandomness factors α equal to 0.2. Since this binary system contains no ions, the only parameters remaining are τ_{35} and τ_{53}. The matching exercise is then a straightforward matter of trial and error, and it gives

$$\tau_{35} = 2.264 \qquad (22)$$

$$\tau_{53} = 5.983 \qquad (23)$$

Next, the HI-H_2O pair also exhibits incomplete miscibility, but in this case the complications due to the presence of the ions must be taken into account. Nevertheless, the analysis can be simplified by making two approximations: (1) Since the amount of water in the HI phase is imperceptibly small, it will be set to zero; and (2) Since HI is known to dissociate almost completely in water, the presence of molecular HI in the aqueous phase will be ignored. Thus, the two phases in the equilibrium calculations are pure liquid HI and a completely dissociated hydriodic acid solution. This simplification reduces the list of unknown ElecNRTL parameters for this system to two, namely $\tau_{ca,5}$ and $\tau_{5,ca}$. Furthermore, the dielectric constant of HI is not needed; the value for H_2O at 393 K is estimated from Lange's Handbook [17] to be 51.

As always, standard state thermodynamic data is needed for all of the species involved, and in this case not everything is readily available. In particular, properties for liquid HI are difficult to find, so they have been computed by combining data for gaseous HI with a value for the heat of vaporization at the normal boiling point and an estimate for the liquid-phase heat capacity from a correlation given by Reid, Prausnitz and Sherwood [18]. Also, properties for the hydronium ion H_3O^+ are obtained by adding the corresponding values for water and the fictitious hydrogen ion H^+.

From [2], the nominal (i.e., pre-dissociation) mole fraction of HI in the H_2O-rich phase is 0.286, and it is easily seen that this is also the mole fraction of I^- ions in the completely dissociated solution. It seems clear that there can be no unique set of values of the two ElecNRTL parameters that will yield the single desired composition. A further

21

complication is that the EQUIL calculations often fail to converge for this problem (for currently unknown reasons); for these cases the free energy minimization must be carried out manually. If $\tau_{ca,5}$ is set to zero, it is found that there is no value of $\tau_{5,ca}$ that will give the desired result. On the other hand, if $\tau_{5,ca}$ is zero, then the correct equilibrium state is achieved for

$$\tau_{ca,5} = -3.16 \tag{24}$$

Unfortunately, EQUIL does not converge for $\tau_{ca,5}$ less than about -2.8.

Since there are no further binary systems to be investigated, the next logical step is to attempt to match the phase envelopes in Figure 8 by adjusting the remaining ElecNRTL parameters. This can in principle be accomplished by selecting a set of parameter values and then using EQUIL to compute the number of coexisting phases (as well as their compositions) at various points on the phase diagram. Needless to say, this will be a time-consuming and perhaps tedious task even if the EQUIL calculations always converge, and it will be utterly impractical otherwise. In light of the convergence failures noted above, it is clear that the robustness of EQUIL must be improved before any further progress can be made.

SUMMARY

The goal of the laboratory phase of this study was to design, fabricate, and operate a pressure vessel to acquire vapor-liquid equilibrium data. The measurements were to include the phase compositions (two liquid phases and the vapor phase) and the vapor pressure for a range of temperatures and initial compositions of the constituents. The experimental work was significantly and negatively affected by greater than anticipated difficulties in constructing a suitable equilibrium cell capable of containing the highly corrosive mixture of iodine, hydriodic acid and water at temperatures of nominally 200°C. Delays in procuring a pressure cell suitable for handling this mixture forestalled this approach. Based on the initial attempt to design a cell for high pressure studies, alternative designs are suggested that may be able to accommodate the stringent requirements necessary to attain thermodynamic equilibrium in this multi-component system while accessing the cell to sample all phases. A Pyrex test cell was assembled and several tests were run at lower temperature and pressure than the original proposal. This cell was operated at nominally 120°C, above the liquidus temperature of iodine, and 40 psi. Samples were collected from the water-rich liquid phase and analyzed for iodine content.

The goal of the computational modeling part of this project was to develop the capability to construct phase diagrams that describe the behavior of the HI-iodine-water system by making enhancements to Sandia's Chemkin package of codes. A four-step approach was adopted to obtain a set of codes that can do the necessary computations. First, the EQUIL code and its STANJAN-based subroutines were adapted to make use of the physical properties provided by the Liquid Chemkin subroutine library. Second, the newly modified EQUIL code was used to construct some representative phase diagrams for other multi-component systems by employing the nonideal-liquid models currently existing in Liquid Chemkin. This demonstrated that the Chemkin suite can model the kinds of complex phase behavior associated with nonideal liquid mixtures, in particular the existence of azeotropes and the phenomenon of phase splitting. Next, the model needed to represent the thermodynamic properties of HI-iodine-water mixtures was added to Liquid Chemkin. Although Liquid Chemkin already had some ability to handle ionic solutions and nonideal mixtures of non-electrolytes, a model that addressed both of these complexities simultaneously was needed. The final step, which involved using the new thermodynamic model to compare the results of EQUIL computations with experimental data in order to evaluate any unknown parameters for the HI-iodine-water system, was not completely successful due to convergence problems in the code. This problem could be overcome with additional effort.

This page intentionally left blank

REFERENCES

1. L. C. Brown, J. F. Funk and S. K. Showalter, "Initial Screening of Thermochemical Water-Splitting Cycles for High Efficiency Generation of Hydrogen Fuels Using Nuclear Power", Sandia National Laboratories, SAND2000-1263 (2000).

2. D. R. O'Keefe, J. H. Norman, L. C. Brown, and G. E. Besenbruch, "GA Technologies Thermochemical Water-Splitting Process Improvements," GA Technologies report GA-A17752 (1985).

3. H. Engels and K. F. Knoche, "Vapor pressures of the system $HI-I_2-H_2O$ and H_2", Int. J. Hydrogen Energy, 11 (11), 703 (1986).

4. M. Roth and K. F. Knoche, "Thermochemical water splitting through direct HI-decomposition from $HI-I_2-H_2O$ solutions", Int. J. Hydrogen Energy, 14 (8), 545 (1989).

5. M. Sakurai, H. Nakajima, K. Onuki and S. Shimizu, "Investigation of 2 liquid phase separation characteristics on the iodine-sulfur thermochemical hydrogen production process", Int. J. Hydrogen Energy, 25, 605-611 (2000).

6. H. Ishikawa, E. Ishii, I. Uehara and M. Nakane, "Studies of Thermochemical Hydrogen Production. VII. Vapor-Liquid Equilibrium for Sulfur Dioxide-Bromine-Hydrobromic Acid-Sulfuric Acid-Water System", Bull. Chem. Soc. Japan, 53 (9), 2510-2513 (1980).

7. L. A. Watts and B. Louie, "Apparatus for Measuring Vapor-Liquid Equilibria and Phase Densities of Complex Aqueous Solutions", Int. J. Thermophys., 21 (5), 1139 (2000).

8. G. Wuster, G. Wozny and Z. Giazitzoglou, "Thermodynamic description of the electrolytic mixed system $HBr-H_2O$ at moderate pressures by use of gas phase p, v, T and total pressure measurements", Fluid Phase Equilibria, 6, 93 (1981).

9. DR2010 Spectrophotmeter Procedures Manual, Mthod 8031, Hach Co., Loveland, CO, 1999.

10. R. J. Kee, F. M. Rupley, J. A. Miller, M. E. Coltrin, J. F. Grcar, E. Meeks, H. K. Moffat, A. E. Lutz, G. Dixon-Lewis, M. D. Smooke, J. Warnatz, G. H. Evans, R. S. Larson, R. E. Mitchell, L. R. Petzold, W. C. Reynolds, M. Caracotsios, W. E. Stewart, and P. Glarborg, CHEMKIN Collection, Release 3.5, Reaction Design, Inc., San Diego, CA (1999).

11. K. S. Chen, G. H. Evans, R. S. Larson, D. R. Noble, and W. G. Houf, "Final Report on LDRD Project: A Phenomenological Model for Multicomponent Transport with Simultaneous Electrochemical Reactions in Concentrated Solutions," SAND2000-0207 (2000).

12. W. C. Reynolds, "STANJAN - Interactive Computer Programs for Chemical Equilibrium Analysis," Stanford University report (1981).

13. J. M. Prausnitz, *Molecular Thermodynamics of Fluid-Phase Equilibria*. Prentice-Hall, Englewood Cliffs, NJ (1969).

14. P. M. Mathias and L. C. Brown, "Thermodynamics of the Sulfur-Iodine Cycle for Thermochemical Hydrogen Production," 68th Annual Meeting of the Society of Chemical Engineers, Japan (2003).

15. C.-C. Chen, H. I. Britt, J. F. Boston, and L. B. Evans, *AIChE J.* 28, 588 (1982).

16. C.-C. Chen and L. B. Evans, *AIChE J.* 32, 444 (1986).

17. J. A. Dean, editor, *Lange's Handbook of Chemistry*, 11th ed. McGraw-Hill, New York (1973).
18. R. C. Reid, J. M. Prausnitz, and T. K. Sherwood, *The Properties of Gases and Liquids*, 3rd ed. McGraw-Hill, New York (1977).
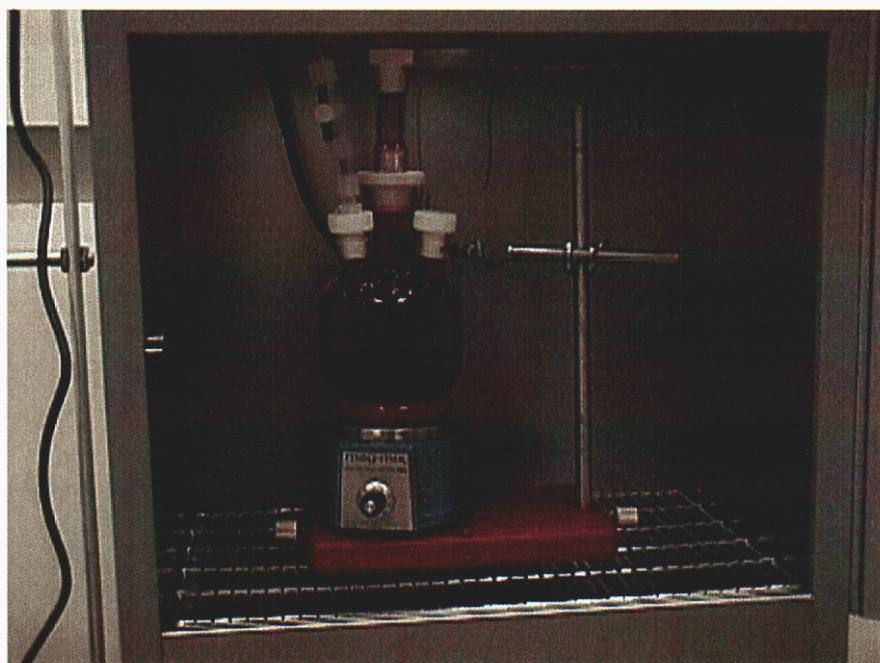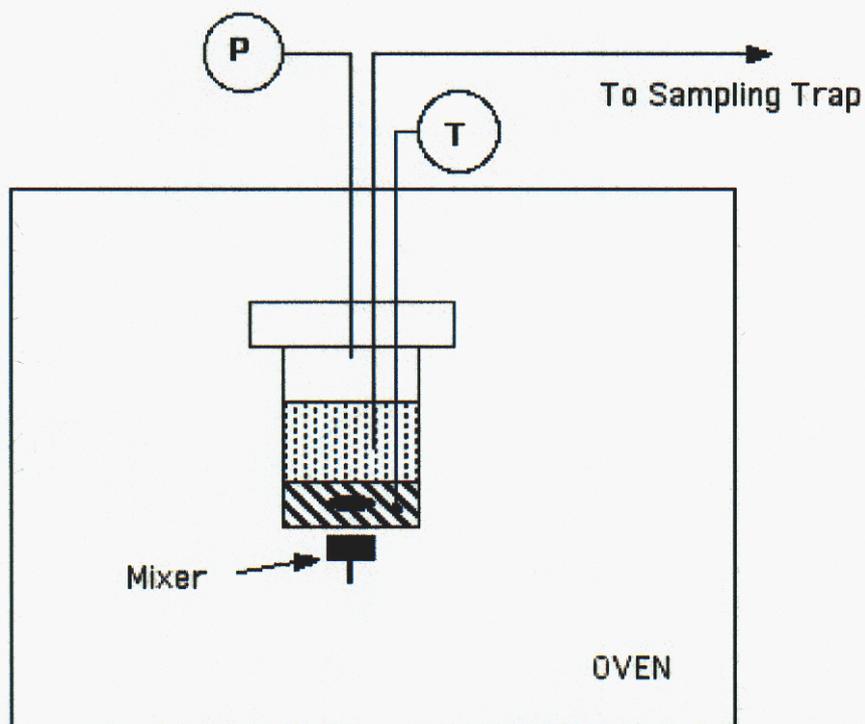
Figure 1. Schematic diagram and photograph of equilibrium cell used for preliminary experiments with the water-hydriodic acid-iodine system.
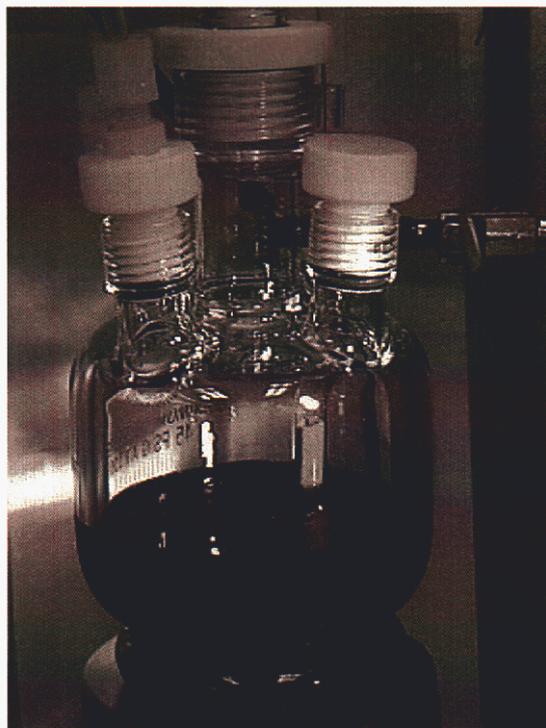
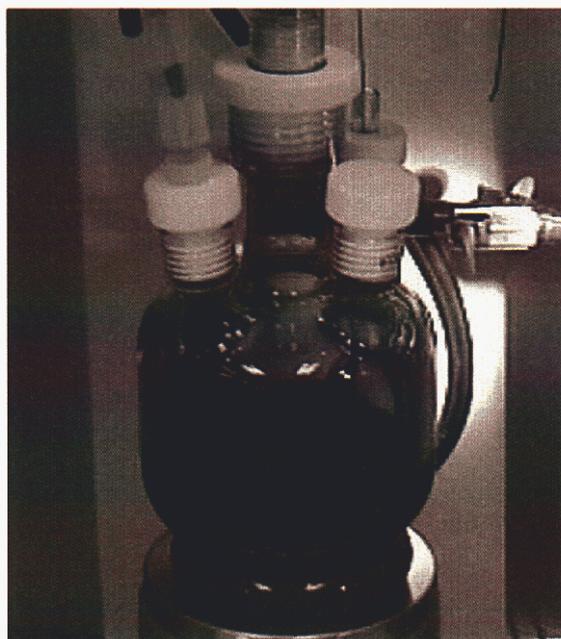Figure 2. Photograph (detail) of equilibrium cell used for preliminary experiments.

Figure 3. Photograph of equilibrium cell showing color density of vapor phase at relatively high HI concentration; compare opacity to Figure 2.
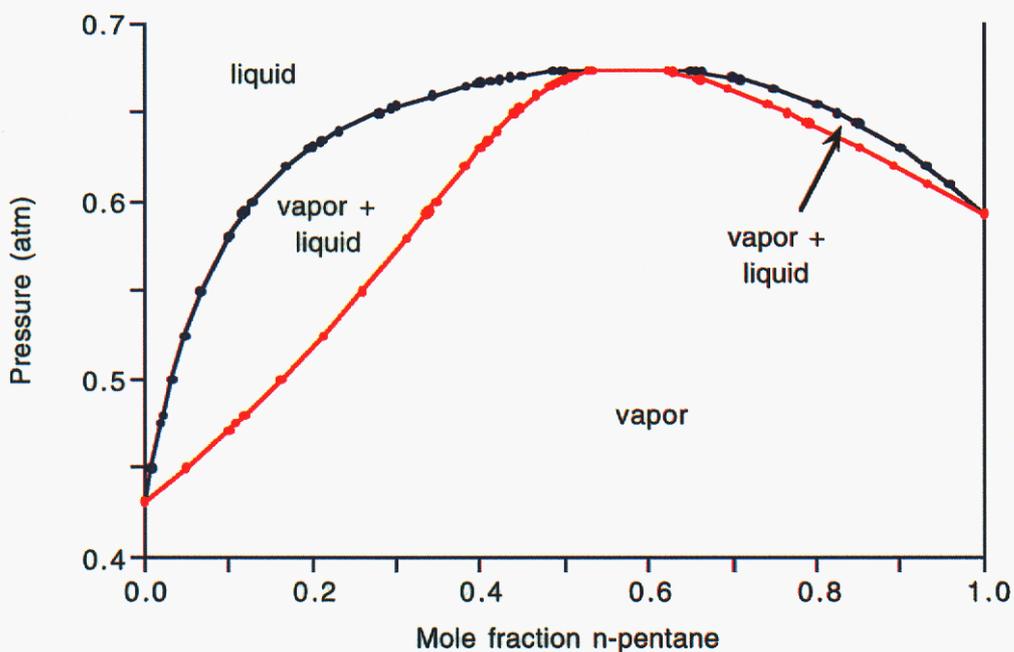
Figure 4. Phase diagram for n-pentane/carbon disulfide at 298.15 K according to regular solution theory.
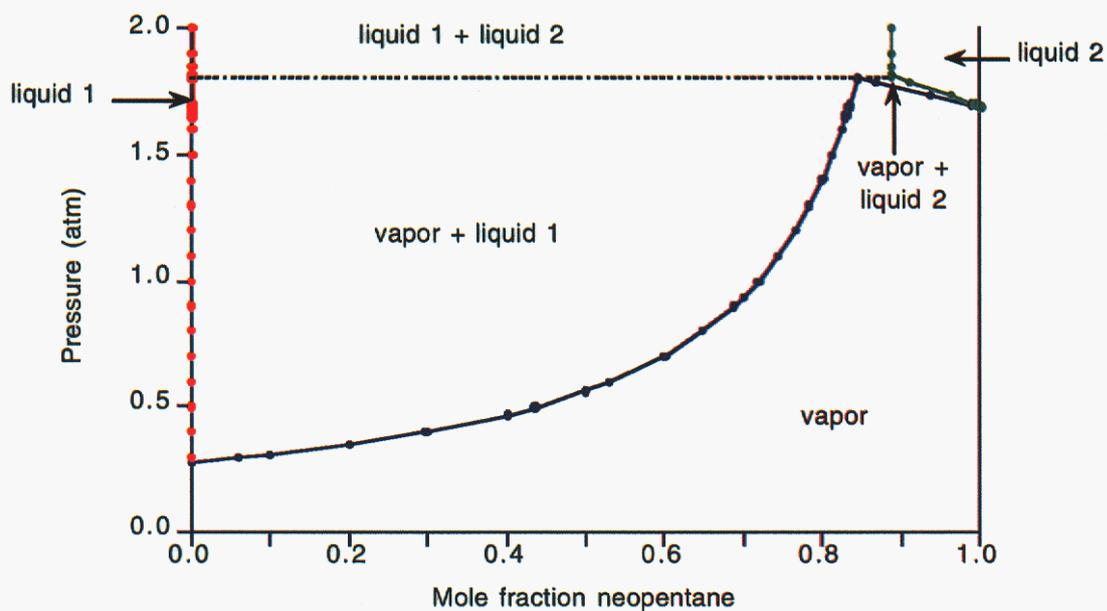

Figure 5. Phase diagram for neopentane-bromine at 298.15 K according to regular solution theory.
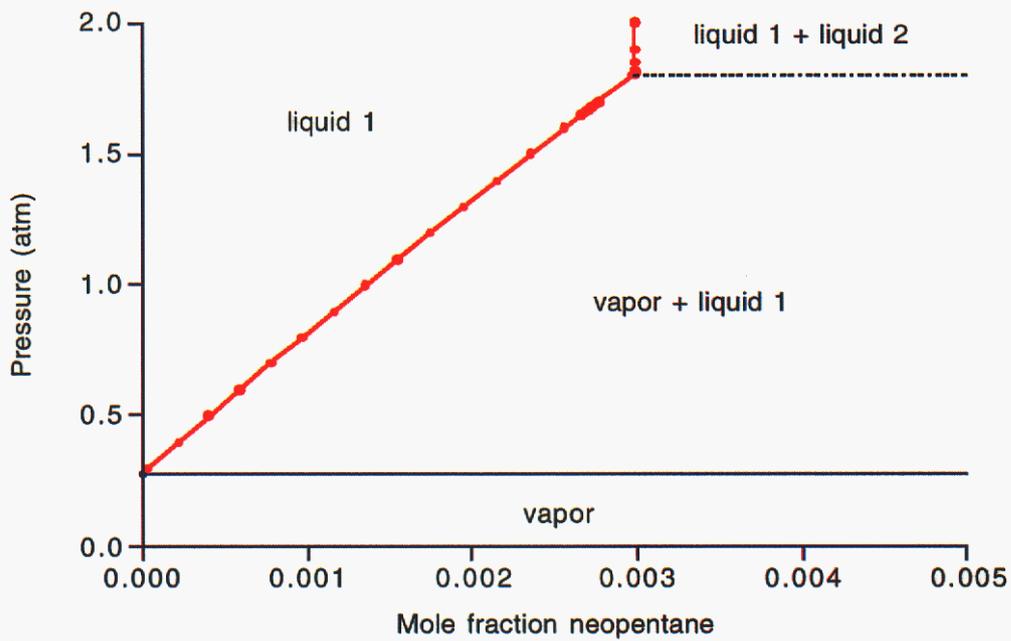
Figure 6. Phase diagram for neopentane-bromine at 298.15 K according to regular solution theory (expanded view).
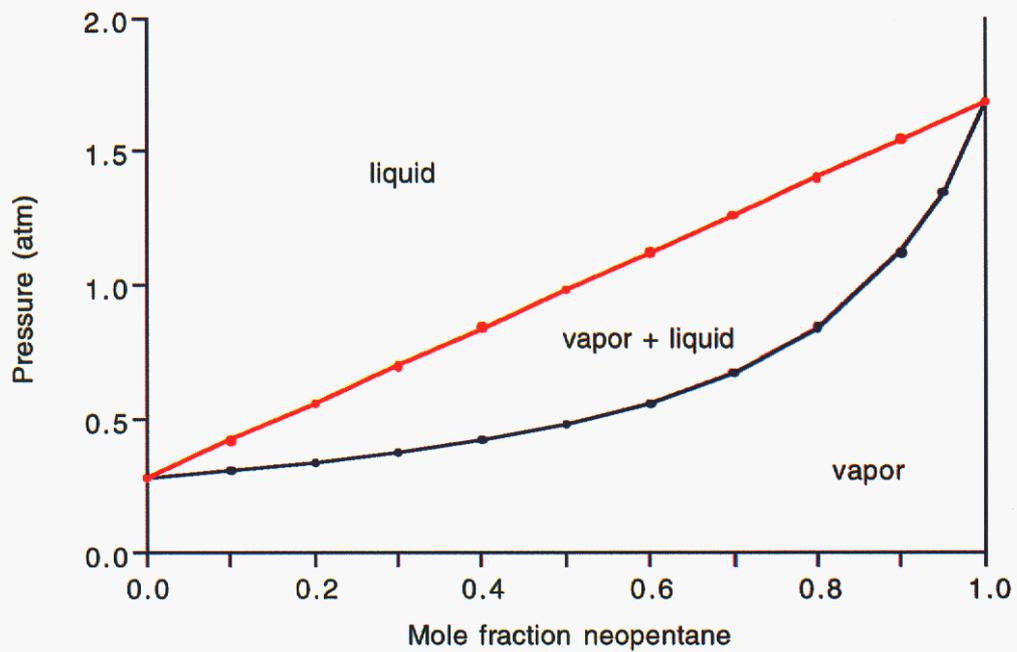

Figure 7. Phase diagram for neopentane-bromine at 298.15 K according to ideal solution theory.
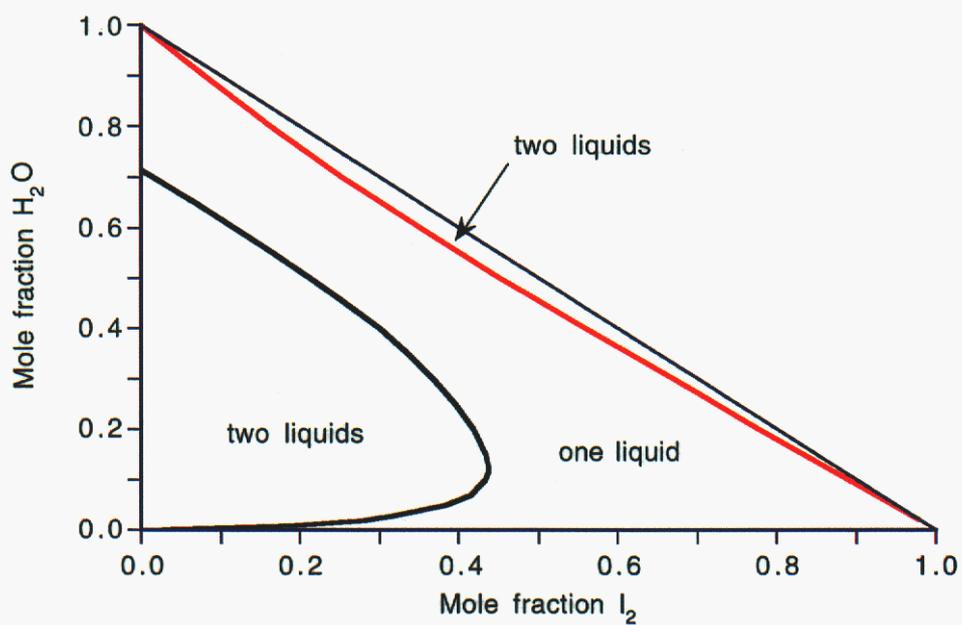
Figure 8. Ternary phase diagram for HI-I$_2$-H$_2$O at 393 K and 4.3 MPa (from O'Keefe [8]).

DISTRIBUTION

Lloyd C. Brown
General Atomics Co.
PO Box 85608
San Diego, CA   92186-5608

James A. Fort
Pacific Northwest National Laboratory
P.O. Box 999 / K7-15
Richland, WA 99352

Ellen Meeks
Reaction Design, Inc.
6440 Lusk Boulevard, Suite D-209
San Diego, CA 92121

1	MS 0727	D. A. Powers, 6870
1	MS 0748	F. Gelbard, 6863
1	MS 0834	K. S. Chen, 9114
1	MS 0834	J. E. Johannes, 9114
1	MS 0834	H. K. Moffat, 9114
1	MS 0889	J. W. Braithwaite, 1832
1	MS 1136	P. S. Pickard, 6872
3	MS 9042	R. S. Larson, 8752
1	MS 9042	C. D. Moen, 8752
1	MS 9053	A. E. Lutz, 8367
3	MS 9403	R. W. Bradshaw, 8762
1	MS 9403	T. J. Shepodd 8762
1	MS 0323	D. L. Chavez, LDRD Office, 1011
3	MS 9018	Central Technical Files, 8945-1
1	MS 0899	Technical Library, 9616
1	MS 9021	Classification Office, 8511, for Technical Library, MS 0899, 9616 DOE/OSTI